TU Delft

Delft University of Technology

# Stand-Alone Broad Frequency Range Charge-Balancing System for Neural Stimulators

Späth, Jana M. ; Kolovou Kouri, Konstantina; Holzapfel, Lukas ; Thewes, Roland ; Giagka, Vasiliki

**DOI**
10.1109/BioCAS58349.2023.10388758

**Publication date**
2023

**Document Version**
Final published version

**Published in**
Proceedings of the 2023 IEEE Biomedical Circuits and Systems Conference (BioCAS)

**Citation (APA)**
Späth, J. M., Kolovou Kouri, K., Holzapfel, L., Thewes, R., & Giagka, V. (2023). Stand-Alone Broad Frequency Range Charge-Balancing System for Neural Stimulators. In *Proceedings of the 2023 IEEE Biomedical Circuits and Systems Conference (BioCAS)* IEEE. https://doi.org/10.1109/BioCAS58349.2023.10388758

**Important note**
To cite this publication, please use the final published version (if applicable).
Please check the document version above.

**Copyright**
Other than for strictly personal use, it is not permitted to download, forward or distribute the text or part of it, without the consent of the author(s) and/or copyright holder(s), unless the work is under an open content license such as Creative Commons.

**Takedown policy**
Please contact us and provide details if you believe this document breaches copyrights.
We will remove access to the work immediately and investigate your claim.

*This work is downloaded from Delft University of Technology.*
*For technical reasons the number of authors shown on this cover page is limited to a maximum of 10.*

*Green Open Access added to TU Delft Institutional Repository*

*'You share, we take care!' - Taverne project*

*https://www.openaccess.nl/en/you-share-we-take-care*

Otherwise as indicated in the copyright section: the publisher is the copyright holder of this work and the author uses the Dutch legislation to make this work public.

# Stand-Alone Broad Frequency Range Charge-Balancing System for Neural Stimulators

Jana M. Späth[1,2], Konstantina Kolovou Kouri[1,3], Lukas Holzapfel[1], Roland Thewes[2], Vasiliki Giagka[1,3]

[1]Fraunhofer Institute for Reliability and Microintegration, Berlin, Germany
[2]Chair of Sensor and Actuator Systems, Technische Universität Berlin, Faculty of EECS, Berlin, Germany
[3]Bioelectronics Section, Dept. of Microelectronics, Delft University of Technology, Delft, The Netherlands

v.giagka@tudelft.nl

2023 IEEE Biomedical Circuits and Systems Conference (BioCAS) | 979-8-3503-0026-0/23/$31.00 ©2023 IEEE | DOI: 10.1109/BioCAS58349.2023.10388758

***Abstract*— Safety is a critical consideration when designing an electrical neural stimulator, given the direct contact with neural tissue. This paper presents the design of a charge balancing system suitable for frequencies up to the kilohertz domain, to be used as an add-on system for stimulators over a wide range of frequencies, also covering nerve conduction blocking. It operates independently of the stimulator timing by continuously sensing the offset voltage, and applying a corrective current to the electrode, using the offset compensation technique. To ensure its stand-alone capability, the system is battery-powered, and includes a safety and start-up circuit. Electrical measurements verified the functionality of the circuit, demonstrating a residual offset of only 0.7 mV for 1 V biphasic pulses at 50 kHz. When tested for 20 kHz biphasic pulse at a 5 V amplitude, the offset was measured at -11.6 mV, which is still within the (commonly used) ±50 mV safety window.**

***Keywords—neural stimulation, active charge balancing, offset compensation, kilohertz frequency alternating current (KHFAC)***

## I. Introduction

Implants for electrical neural stimulation can target various nerves in the human body to treat diseases caused by malfunctions of the nervous system [1]. Neural stimulators can excite and block neural activity depending on the frequency of the applied stimulation pattern, which is often a biphasic pulse. For excitation, frequencies below 500 Hz are commonly used, while blocking of neural activity occurs in the kilohertz range; certainly above 1 kHz, mainly above 5 kHz [2]. This method is called kilohertz frequency alternating current (KHFAC) stimulation, as described in [2], and is the more common approach to achieving nerve conduction block.

Modulating neural activity through electrical signals is possible through an electrode that provides the interface to the nerve tissue and allows for the necessary charge transfer. This charge transfer results in chemical reactions at the electrode-tissue interface (ETI), which can be reversible or irreversible [3]. These processes are represented in an electrical model for the ETI consisting of the spreading resistance $R_S$ (approx. 1 kΩ-10 kΩ), the double layer capacitance $C_{DL}$ (approx. 100 nF-1 µF) and the faradaic resistance $R_F$ (approx. 100 kΩ-10 MΩ), resulting in an overall high impedance [4, 5]. During a biphasic pulse, the first phase triggers neural activation, while the second phase serves as an initial charge-balancing technique, reversing the reversible part of these reactions. The amount of charge lost in irreversible processes depends on the DC voltage level at the ETI at the end of the biphasic pulse, also known as the electrode offset voltage [6]. The electrode offset voltage occurs due to mismatches or offsets in the stimulator's output signal, or nonlinearities at the ETI [4]. When more charge is transferred for one phase of the biphasic pulse versus the other, the $C_{DL}$ is charged accordingly. If the time between the pulses is too short to allow for gradual and slow discharging, the offset voltage increases with every period. If this offset is outside a defined safety window of ±50 mV [5] or ±100 mV [7], it can induce damage to the electrode and the tissue. Therefore, achieving charge balancing (CB) at the ETI and, thus, a stable offset voltage within the given limits, is an essential part of the stimulator system design.

Most commercially available stimulators include a passive charge balancing approach, which can be insufficient, especially for the frequency range of signals for nerve conduction blocking [2]. Passive charge balancing has no feedback from the electrode voltage. A conventional method is electrode shorting, where electrodes are shorted to allow for discharging between biphasic pulses [8]. This method is insufficient for KHFAC signals because the discharge time can be too short. The most commonly used method is to place a DC blocking capacitor between the stimulator and each electrode, thus establishing a high-pass filter [9]. However, [9] suggests that the DC blocking capacitor introduces an additional offset voltage that cannot be controlled by the stimulator.

Active CB approaches include a feedback pathway that provides information about the offset voltage at the electrode site. Most approaches focus on stimulation patterns used to excite neural activity and, therefore, on frequencies below 500 Hz. These can be divided into CB methods that modify the stimulation pattern in timing [4] or amplitude [10, 11], when there is access to its programmability, and CB methods that inject charge in addition to the stimulation pulse [12]. A popular method of charge injection is pulse insertion, as described in [5]. If the measured offset voltage is not within the given safety limits, predefined charge packages are applied until the voltage is again within the safety window. An alternative charge injection approach presented in [7] is the offset compensation (OC). A control system determines an offset current that is applied either permanently or only during a dedicated phase [7] to minimize the electrode offset voltage.

Active CB systems measure the electrode offset voltage either continuously [13] or in a discrete manner by

Authorized licensed use limited to: TU Delft Library. Downloaded on February 01,2024 at 07:39:16 UTC from IEEE Xplore. Restrictions apply.

sampling after the biphasic pulse [7]. A continuous measurement system must be capable of handling high voltages and should provide a high input impedance so that no current leaks into the system instead of the electrode. This is not necessary if the system measures in a discrete manner and is disconnected during the stimulation pulses.

This paper proposes a stand-alone CB system that can be used as a plug-in component on any stimulator. The system is compatible with a broad range of frequencies and is particularly beneficial for the more demanding KHFAC applications. Section II presents the proposed system, focusing on the core CB circuit, the safety circuit, and the start-up circuit, followed by the system validation in section III. A conclusion in section IV summarizes the results.

## II. Proposed System

The proposed system consists of a core circuit, divided into a measurement part and a charge injection part (Fig. 1). A voltage follower, integrator, and amplifier are used to continuously monitor the electrode offset voltage. A voltage-controlled current source (VCCS) converts the electrode offset voltage into a current that is added to the stimulator current, the sum of which is the final current applied to the electrode. Fig. 2 illustrates the OC method in the example of a biphasic stimulation pulse with a 20 % amplitude mismatch between the two phases. Finally, a safety and start-up circuit ensure reliable operation. The system is built using commercially available components, thus ensuring its reproducibility and ease of access.

### A. Charge Balancing Circuit

To design a system capable of charge balancing for KHFAC stimulation, a focus on the short duration between pulses (interpulse delay) and the high-frequency components of the signal, which result from the kilohertz frequency range of the biphasic pulses, is required. A continuous measurement and OC scheme allow independency from the stimulator timing and the duration of the interpulse delay. As the edges of the biphasic pulses for KHFAC come with high-frequency components, it is important to ensure a sufficiently high input impedance, compared to the impedance of the electrode, to prevent leakage currents.

Measuring the electrode offset voltage is an important first step within the feedback loop of the proposed CB system (Fig. 3). The design here uses a simple voltage follower to provide a copy of the electrode voltage to the subsequent circuitry, and to offer a high input impedance. Sufficient gain bandwidth (GBW) and slew rate (SR) are required for the operational amplifier (OpAmp) to ensure linearity for the stimulation signal's frequency range.

Reference [13] uses a low-pass filter (LPF) to integrate the electrode voltage over several stimulation periods, to continuously determine the offset voltage. The CB system proposed here follows the recommendation of [14, pp. 26-27], suggesting that integration is more accurate when an active integrator with an OpAmp is used. The integrator has a time constant defined by $R_{int}$ and $C_{int}$, which needs to be larger than the period of the biphasic pulse. For nerve conduction block stimulation frequencies between 1 kHz and 20 kHz, a time constant of 10 ms results in 10-200 integrated periods. A buffered trimming circuit is connected to the non-inverting input of the integrator's OpAmp. A trimming circuit is typically used to solve offset problems. Furthermore, it allows the user to add a defined offset to the electrode voltage, similar to the implementation in [13]. As [15] suggests, an offset voltage of up to several hundreds of millivolts results in better electrode performance for some electrode materials, such as Iridium Oxide, due to the improved charge injection capacity. The integrator is followed by a non-inverting amplifier. The amplification of the integrator output results in a faster settling of the circuit by adding a gain to the feedback. A potentiometer (R1) permits the user to adjust this gain.

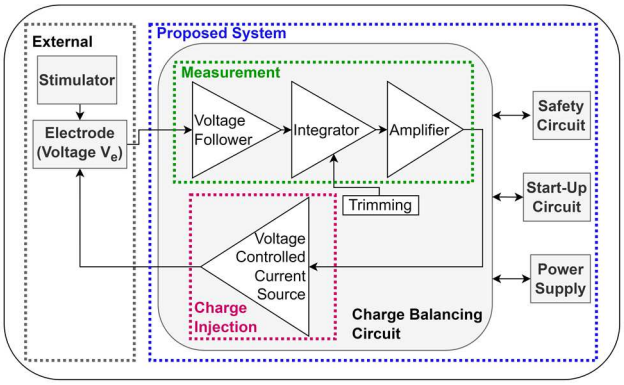


Fig. 1. Block diagram of the complete proposed CB system. The proposed system uses the integrator output, which provides the electrode offset voltage, to drive a voltage controlled current source (VCCS). The battery management system supplies all components with ±12 V. A safety circuit prevents system malfunction in case of saturation. Dedicated switches and a relay provide a safe system start-up.

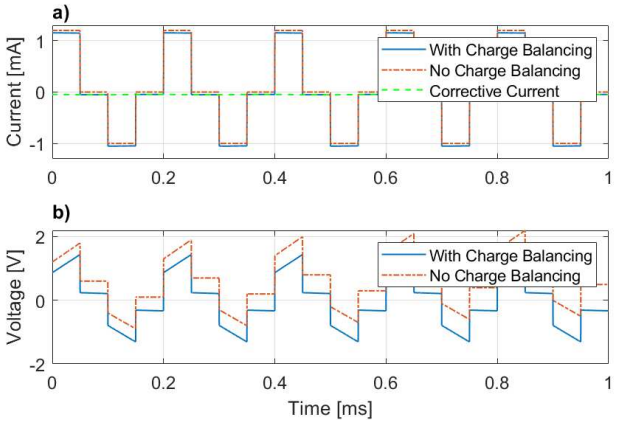


Fig. 2. a) Balanced and unbalanced currents as a function of time b) Electrode voltage for balanced and unbalanced pulse patterns as a function of time. For this simulation, a 20 % mismatch between the anodic and cathodic phases' amplitudes is introduced.

The amplified integrator output drives a VCCS connected to the electrode. A commonly used VCCS is the Howland current source (HCS). One issue that is often overlooked when using the HCS in stimulators, as in [13], is the low output impedance at high frequencies. The buffered HCS (Fig. 3) improves the output impedance by zeroing the feedback current through $R_{15}$. Equally important is finding matching resistors for $R_{12}$-$R_{15}$, as a mismatch results in lower output impedance. Therefore, a resistor network is used. Furthermore, the frequency-dependent gain of the OpAmps, given with the component's GBW, results in a decreasing output

Authorized licensed use limited to: TU Delft Library. Downloaded on February 01,2024 at 07:39:16 UTC from IEEE Xplore. Restrictions apply.

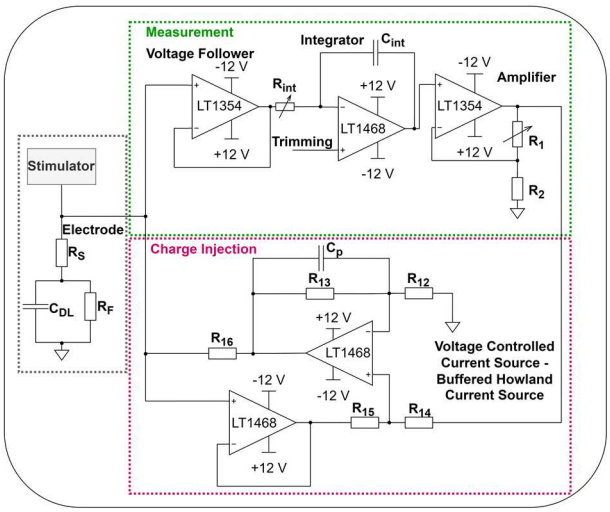


Fig. 3. Schematic of the system's core circuit consisting of five OpAmps. The electrode model represents one electrode consisting of the spreading resistance $R_S$, the faradaic resistance $R_F$ and the double layer capacitance $C_{DL}$. $R_{int}$=1-100 kΩ, $C_{int}$=1 µF, $R_1$=1-100 kΩ, $R_2$=1 kΩ, $R_{12}$-$R_{16}$=10 kΩ, $C_p$=5 pF.

impedance of the HCS with increasing frequency. This leads to a high GBW requirement for the chosen OpAmp. For this HCS structure, the resistor at the output, $R_{16}$, defines the ratio of input voltage to output current, but also contributes to the output impedance.

### B. Safety Circuit

The safety circuit is implemented to handle errors due to voltage follower saturation at high input voltages. Turning off the power supply is an easy way to turn off the system. Therefore, the power management system includes the dual-supply IC twice; one that is continuously operated and one that is controlled by the safety circuit. A window comparator, along with a logic circuit, drives the enable pin of the safety dual-supply IC. When disabled, the HCS, amplifier, and integrator are turned off to ensure that no erroneous offset current is applied to the ETI.

### C. Start-Up Circuit

Two issues arise when starting up the circuit. First, the safety dual supply does not provide the positive and negative voltages with equal SR at start-up. This creates an imbalance in the system, resulting in an incorrect output current at the HCS during start-up. Furthermore, charge is stored in the integrator capacitor due to offset and bias currents [14, pp. 230-231]. The charged capacitor causes an additional error, and overshoot oscillations may occur at start-up. Therefore, analog switches short-circuit the capacitor and connect the integrator's OpAmp input to ground to ensure discharge until the system is powered up. In addition, a reed relay connects the electrode to ground until the system is adequately powered up. The analog switches and the reed relay are normally closed and open with the signal generated by the start-up circuit.

## III. System Validation

### A. Test Setup

The validation of the CB system and the additional safety and start-up circuit requires a setup that includes an arbitrary current source to provide for the stimulation

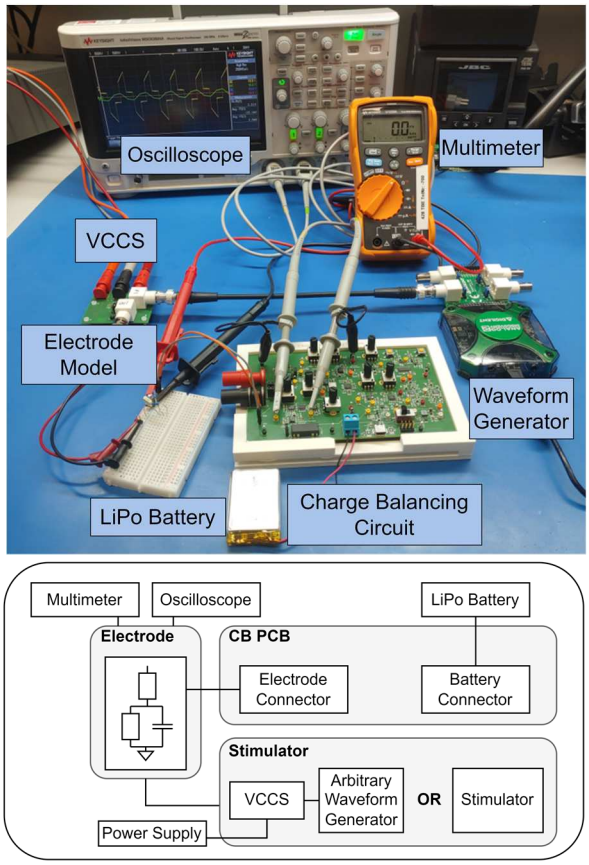


Fig. 4. a) Test setup with VCCS allowing for a high degree of flexibility in measurements. b) Schematic of the test setup pointing out the connections between all used instruments.

signal, an electrode model, and additional measurement equipment, as Fig. 4 shows. An arbitrary function generator (Analog Discovery 2) followed by a VCCS allows for the flexible simulation of mismatches or offsets to test the efficacy of the developed CB system. The VCCS is the same HCS as used in the CB system with a transconductance of 1 mS, resulting in 1 mA output current for 1 V input voltage. An electrode model consisting of two resistors and one capacitor allows for controlled testing with $R_S$=1 kΩ, $R_F$=1 MΩ, and $C_{DL}$=100 nF, resulting in a well-defined impedance. The DC voltage setting on the multimeter (Keysight U1233A) measures the offset of the stimulation pulses in the kilohertz range. An oscilloscope (InfiniiVision MSOX2024A) measures time-continuous signals.

### B. Measurement Results

To show the functionality of the OC scheme, a constant offset is added to the stimulator current. As Fig. 5 shows the stimulator current, which is a biphasic pulse with 1 mA amplitude and a frequency of 5 kHz, is shifted by 200 µA. The corrective current has the expected value of -200 µA, resulting in the charge-balanced electrode current.

A more realistic scenario causing a charge imbalance is a mismatch between the cathodic and anodic phases of a stimulation pulse. To evaluate the capabilities of the CB system, a mismatch of 10 % is applied to the biphasic pulse. The electrode offset voltage is measured for different pulse frequencies and amplitudes, as Fig. 6 shows. The system keeps the offset voltage below 0.7 mV

Authorized licensed use limited to: TU Delft Library. Downloaded on February 01,2024 at 07:39:16 UTC from IEEE Xplore. Restrictions apply.

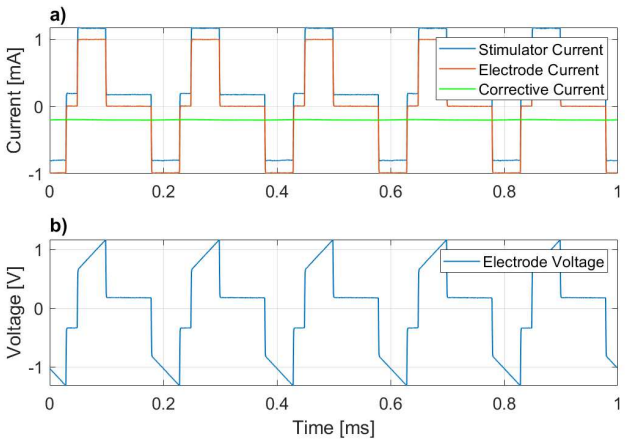


Fig. 5. a) Stimulator, electrode, and corrective current as a function of time with the corrective current adapting to the offset, so that the current through the electrode, which is the sum of the stimulator and corrective current, does not have an offset. b) Charge-balanced electrode voltage as a function of time.

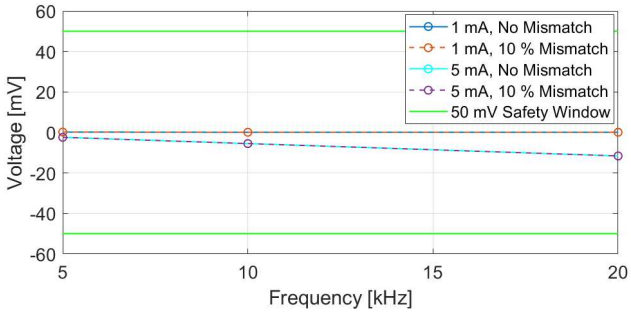


Fig. 6. Electrode offset voltage as a function of frequency depending on the amplitude and frequency of the applied pulses.

for a pulse amplitude of 1 mA current, resulting in approx. 1 V for up to 50 kHz. For a voltage amplitude of 5 V for a frequency of 20 kHz, the offset is 11.6 mV, which is well within the safety window. It is important to note, that the offset voltage measurements are the same for a signal with and without a 10 % mismatch, indicating the efficacy of the CB system for the mismatched case.

The time constant of the feedback loop influences the shape of the corrective current and the start-up behavior, as Fig. 7 shows. Again an offset of 200 µA is added to the VCCS signal. Now the feedback loop time constant, which consists of the HCS's transconductance (0.1 mS), the amplifier's gain (93 V/V), and the integrator's time constant, is varied by setting different integrator time constants. Fig. 7 shows how the corrective current changes accordingly: a smaller time constant increases its peak-to-peak value, influencing the electrode voltage shape.

The initial settling of the corrective current at start-up also depends on the feedback loop's time constant (Fig. 7). A reduced time constant results in faster-settling behavior and a smaller number of overshoots. Therefore, the time constant should be adjusted to the requirements of the application. Adapting the time constant also allows to extend the frequency range over which the system can be used. If the feedback loop is slow compared to the signal's frequency and amplitude, the system is not stable. With an adapted time constant, the system has been tested for frequencies as low as 20 Hz. A comparison to other CB systems in Table 1 shows the achieved quality for this high

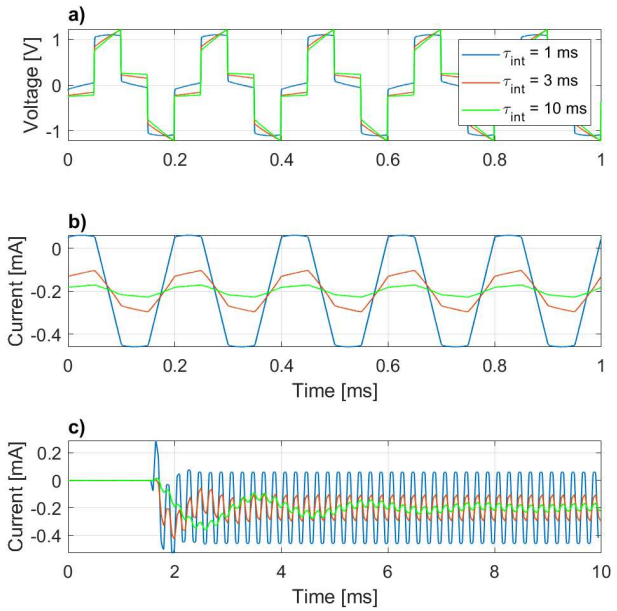


Fig. 7. a) Electrode voltage, b) amplitude of corrective current, and c) corrective current during start-up phase as a function of time for various feedback loop time constants.

TABLE I. COMPARISON BETWEEN EXISTING SYSTEMS

| **Reference** | [5] | [13] | [10] | *This work* |
|---|---|---|---|---|
| ***CB Method*** | Pulse Insertion | Offset Comp. | Pulse Adjustment; Inter-Pulse Current Insertion | *Offset Comp.* |
| ***Frequency [kHz]*** | 3.3[a] | <0.1 | 0.1 | *<50* |
| ***Residual Voltage [mV]*** | ±50 @ 3.3 kHz[a]/ ±15 V | N.A. | ±4 @ 100 Hz/1 V | *±12 @ 20 kHz/5 V, ±0.7 @ 50 kHz/1 V* |
| ***Integrated*** | Yes | No | Yes | *No* |

[a] Figure 2.4.6 in [5]

frequency range regarding the residual voltage. Since the residual voltage depends on various parameters, the given frequency and voltage amplitude of the pulse pattern improve compatibility.

## IV. CONCLUSION

The presented offset compensation system achieves a precise charge-balancing for signals in a broad frequency range up to 50 kHz, while allowing for a stand-alone, stimulator-independent operation. The influence of the corrective current on the waveform is evaluated, as well as the start-up behavior. The system can operate as a plug-in for any stimulator, and is particularly suited for nerve conduction block applications. Future work will further evaluate the relation between the stimulation frequency and amplitude, and the CB system's feedback loop time constant.

## REFERENCES

[1] Y. Liu et al., "Bidirectional Bioelectronic Interfaces: System Design and Circuit Implications," *IEEE Solid-State Circuits Magazine*, vol. 12, no. 2, pp. 30–46, June 2020. doi: 10.1109/MSSC.2020.2987506.

Authorized licensed use limited to: TU Delft Library. Downloaded on February 01,2024 at 07:39:16 UTC from IEEE Xplore. Restrictions apply.

[2] K. L. Kilgore and N. Bhadra, “Reversible nerve conduction block using kilohertz frequency alternating current,” *Neuromodulation : journal of the International Neuromodulation Society*, vol. 17, no. 3, pp. 242–255, April 2014. https://doi.org/10.1111/ner.12100

[3] D. R. Merrill, M. Bikson, and J. G. Jefferys, “Electrical stimulation of excitable tissue: Design of efficacious and safe protocols,” *Journal of Neuroscience Methods*, vol. 141, no. 2, 2005, pp. 171–198. doi:10.1016/j.jneumeth.2004.10.020

[4] R. Guan, P. G. Zufiria, V. Giagka, and W. A. Serdijn, “Circuit Design Considerations for Power-Efficient and Safe Implantable Electrical Neurostimulators,” *2020 IEEE 11th Latin American Symposium on Circuits & Systems (LASCAS)*, vol. 11, pp. 1–4, February 2020. doi: 10.1109/LASCAS45839.2020.9068975.

[5] M. Ortmanns, N. Unger, A. Rocke, M. Gehrke and H. J. Tietdke, “A 0.1mm$^2$, Digitally Programmable Nerve Stimulation Pad Cell with High-Voltage Capability for a Retinal Implant,” *2006 IEEE International Solid State Circuits Conference – Digest of Technical Papers*, pp. 89-98, February 2006. doi: 10.1109/ISSCC.2006.1696037.

[6] K. Kolovou-Kouri, S. Soloukey, B. S. Harhangi, W. A. Serdijn, and V. Giagka, “Dorsal Root Ganglion (DRG) Multichannel Stimulator Prototype Developed for Use in Early Clinical Trials,” *Proc. IEEE Conf. on Neural Eng. (NER) 2021*, Virtual, May 2021. doi: 10.1109/NER49283.2021.9441101.

[7] K. Sooksood, T. Stieglitz, and M. Ortmanns, “An active approach for charge balancing in functional electrical stimulation,” *IEEE Transactions on Biomedical Circuits and Systems*, vol. 4, no. 3, pp. 162–170, June 2010. doi: 10.1109/TBCAS.2010.2040277.

[8] V. Giagka, C. Eder, N. Donaldson, and A. Demosthenous, “An Implantable Versatile Electrode-Driving ASIC for Chronic Epidural Stimulation in Rats,” *IEEE Transactions on Biomedical Circuits and Systems*, vol. 9, no. 3, pp. 387-400, June 2015. doi: 10.1109/TBCAS.2014.2330859.

[9] M. N. van Dongen and W. A. Serdijn, “Does a coupling capacitor enhance the charge balance during neural stimulation? An empirical study,” *Medical & biological engineering & computing*, vol. 54, no. 1, pp. 93–101, January 2016. doi:10.1007/s11517-015-1312-9

[10] F. Eshaghi, E. Najafiaghdam and H. Kassiri, “A 24-Channel Neurostimulator IC With Channel-Specific Energy-Efficient Hybrid Preventive-Detective Dynamic-Precision Charge Balancing,” *IEEE Access*, vol. 9, pp. 95884-95895, July 2021. doi: 10.1109/ACCESS.2021.3094766.

[11] N. Butz, A. Taschwer, S. Nessler, Y. Manoli and M. Kuhl, “A 22 V Compliant 56 μ W Twin-Track Active Charge Balancing Enabling 100% Charge Compensation Even in Monophasic and 36% Amplitude Correction in Biphasic Neural Stimulators,” *IEEE Journal of Solid-State Circuits*, vol. 53, no. 8, pp. 2298-2310, August 2018. doi: 10.1109/JSSC.2018.2828823.

[12] A. Urso, V. Giagka, M. van Dongen, and W. A. Serdijn, “An ultra-high-frequency 8-channel neurostimulator circuit with 68% peak power efficiency’,” *IEEE Transactions on Biomedical Circuits and Systems*, vol. 13, no. 5, pp. 882–892, October 2019. doi: 10.1109/TBCAS.2019.2920294.

[13] M. Schuettler, M. Franke, T. B. Krueger, and T. Stieglitz, “A voltage-controlled current source with regulated electrode bias-voltage for safe neural stimulation,” *Journal of Neuroscience Methods*, vol. 171, no. 2, pp. 248–252, June 2008. doi: 10.1016/j.jneumeth.2008.03.016.

[14] P. Horowitz and W. Hill, The art of electronics, 3rd ed. New York: Cambridge Universty Press, 2015.

[15] S. F. Cogan, “Neural stimulation and recording electrodes,” *Annual Review of Biomedical Engineering*, vol. 10, pp. 275–309, April 2008. doi: 10.1146/annurev.bioeng.10.061807.160518.

Authorized licensed use limited to: TU Delft Library. Downloaded on February 01,2024 at 07:39:16 UTC from IEEE Xplore. Restrictions apply.